Prototype Design and Performance Verification of a Movable Handrail for Extravehicular Activity of Astronaut

LIU Junliang[1], *FU Hao*[1,2*], *WANG Zhe*[1], *FAN Ziqi*[1], *GUO Tao*[1]

1. Beijing Institute of Spacecraft Environment Engineering, Beijing 100094, P. R. China;
2. School of Mechatronics Engineering, Harbin Institute of Technology, Harbin 150001, P. R. China

(Received 6 March 2023; revised 3 June 2023; accepted 10 July 2023)

Abstract: In view of the problem that the extravehicular fixed handrail is difficult to meet astronaut's complex extravehicular activity (EVA) needs, we propose a new design of movable handrail to benefit the EVA of astronauts. Specifically, we fully consider the hand force characteristics of astronauts in the pressurized spacesuit and design the parameters for geometric dimension and spring stiffness of each operating component in the movable handrail. In addition, in order to meet the needs of astronauts to operate the movable handrail with one hand during EVA, each operating component can be self-lock. Dynamics simulation analysis of each operating component is performed with ADAMS software. Simulation results show that operating components can be locked under appropriate operating force. We develop an engineering prototype of the extravehicular movable handrail based on the design and analysis result. Experimental verifications are carried out in terms of function, environment and ergonomics, which show that the proposed prototype can not only realize the clamping of the extravehicular fixed handrail but also freely adjust its own length and angle. In addition, the measured operating force is basically consistent with the theoretical value, and there is little change in the operating force before and after the force and thermal environment tests. All these experiments show that the proposed movable handrail has good adaptability to low-orbit environment of the space station.

Key words: extravehicular activity (EVA); extravehicular movable handrail; mechanism design; ergonomics

CLC number: V467 **Document code:** A **Article ID:** 1005-1120(2024)01-0107-15

0 Introduction

The extravehicular handrail is an important auxiliary equipment for astronaut extravehicular activity (EVA)[1-3], which can significantly assist the astronaut's extravehicular behavior and support the maintenance operations. With the extravehicular handrail, a reliable connection between astronauts and the space station can be achieved, which is important to protect the safety of the astronauts during the EVA process. Typically, extravehicular handrails can be divided into two types: The fixed handrail and the movable handrail. Currently, the astronauts of the international space station use the fixed handrail to carry out extravehicular operations. With the constraint of the rocket launch envelope, the height of the fixed handrail cannot be very high. However, the expanded relay antenna and solar wing are much higher than the surface of the space station cabin. That means when carrying out such large inertia extravehicular equipment maintenance tasks, there are at least two astronauts required to cooperate with each other. The astronauts on the robotic arm can achieve appropriate operating positions and body posture by adjusting the robotic arm. However, the astronaut on the surface of the cabin cannot grasp the fixed handrail, which may easily lead to the failure of the task. The extravehicular movable handrail can overcome this drawback by its telescopic length

*Corresponding author, E-mail address: fuhao2015@163.com.

How to cite this article: LIU Junliang, FU Hao, WANG Zhe, et al. Prototype design and performance verification of a movable handrail for extravehicular activity of astronaut[J]. Transactions of Nanjing University of Aeronautics and Astronautics, 2024,41(1):107-121.

http://dx.doi.org/10.16356/j.1005-1120.2024.01.009

and adjustable angle. It can change different gestures to make sure the astronauts achieve a comfortable operating position, which significantly enlarges the activity range of the astronauts on the surface of the space station. In summary, the extravehicular movable handrail is an important extension of the fixed handrail, which plays an increasingly important role in the on-orbit construction and extravehicular maintenance of China's space station.

Newman et al.[4] in National Aeronautics and Space Administration (NASA) have developed an auxiliary device for the extravehicular mobility unit (EMU), which is convenient for astronauts to achieve self-dressing. It can be connected and separated from the fixed handrail, and the ball pair and sliding pair are used to adjust the position and attitude of the end mirror, which plays an important role in the early maintenance of the international space station. In 1989, Lyndon et al.[5] proposed and developed a body restraint tether for EVA. The tether connects the extravehicular fixed handrail with the Mini Work Station at the waist of the astronaut through a semi-rigid damping rod to realize the adjustment of the astronaut's positions and angles. It can help astronauts reach the operating position suitable for extravehicular operations, which plays an important role in the on-orbit maintenance of the Hubble telescope[6-7]. Some functions of the above-mentioned extravehicular auxiliary equipment are consistent with the extravehicular movable handrail. For example, they both require the ability to connect with the fixed handrail and adjust the angle and length. However, the angle adjustment and locking of the above equipment are realized by friction, which may lead to problems such as low load, poor stability and short working life. In this paper, to tackle this issue, we creatively put forward a design of extravehicular movable handrail to greatly expand the operation range of astronaut EVA, which has the advantages of strong bearing capacity, good stability and long working life.

Compare with the handrail inside the space station, there are significant differences in the use environment and astronaut clothing status. The space station flies in low orbit at an altitude of 300—500 km. The environmental conditions outside the space station are high vacuum, microgravity, temperature alternation and a large amount of cosmic radiation[8]. Therefore, the friction performance of motion pair contact surface of the extravehicular movable handrail needs to be specially designed to prevent excessive operating force of the activity mechanism from causing astronauts to be unable to operate. In the microgravity environment, it needs to have the function to prevent drifting on the rail. When the astronauts wear extravehicular spacesuit, their physical flexibility is greatly constrained, and the joint resistance moment of their upper limbs and spacesuit gloves can reach up to 20% of the corresponding joint muscle moment of the human body. For example, the adduction/abduction of the shoulder joint is not more than 60°, and the maximum movement moment is not more than 21 N·m. Compared with astronauts without extravehicular spacesuits, the activity ability and range of the astronauts decrease significantly[9]. The sizes of fingers and palms of the spacesuit gloves are larger than those of ordinary gloves, which makes the buttons, handles, paddles, and other parts of the human-machine operation interfaces of the extravehicular movable handrail larger. Compared with bare-hand operation on the ground, the tactile sensitivity of palms and fingers inside the spacesuit glove will decrease. Therefore, the operating force range of each operation switch needs to be quantitatively designed.

1 Prototype Design

The extravehicular movable handrail is composed of fixed clamping component, angle adjusting component, length adjusting component and auxiliary handle, as shown in Fig.1. Among them, the fixed clamping component integrates the functions of clamping, pressing and locking together, which can maintain a highly reliable connection with the extravehicular fixed handrails. It can provide a convenient and stable mechanical interface between the extravehicular movable handrail and the space station. The angle adjusting component can realize multi-angle adjustment within the semi conic enve-

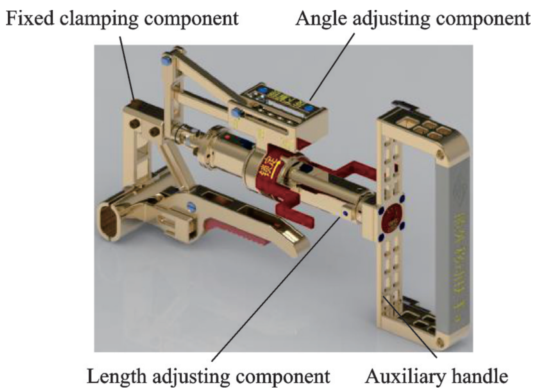

Fig.1 Structure diagram of the extravehicular movable handrail

lope with the fixed handrail clamping point as the center, so as to meet the requirements of different extravehicular maintenance operation positions of astronauts. The length adjusting component can adjust the distance between the auxiliary handle and the space station, so that astronauts can carry out maintenance at different heights. The auxiliary handle is designed for astronauts to grasp the handrail and it also provides an interface for astronauts to take it out of the cabin.

In order to meet the maintenance requirements of space station equipment at different heights and positions, the length adjustment range of the extravehicular movable handrail is designed to be between 398 mm and 558 mm. The angle adjustment range is designed within the half cone with a cone angle of 36°. Therefore, the outer envelope size of the extravehicular movable handrail in the shortened state is 398 mm × 114 mm × 234 mm. The design mass of the extravehicular movable handrail is 2.974 kg.

The mechanism diagram of the extravehicular movable handrail is shown in Fig.2. The fixed clamping component adopts the working principle of eccentric cam pressing and ratchet reverse self-locking. There exists eccentricity between the eccentric cam shaft center and the geometric center. The ratchet wheel and pawl are hinged with the rotating shaft and the eccentric cam, respectively, so that the eccentric cam can only rotate in one direction. When the astronaut rotates the eccentric cam in the forward direction, the contact surface of the cam

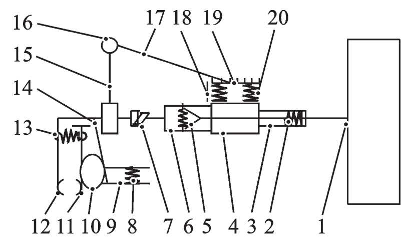

1—Auxiliary handle; 2—Bevel pin self-locking mechanism; 3—Inner rod; 4—Rack base; 5—Bevel pin mechanism; 6—Outer rod; 7—Cardan; 8—Pawl compression spring; 9—Pawl; 10—Eccentric cam; 11—Movable clamp; 12—Fix clamp; 13—Drag spring; 14—Ratchet wheel; 15—Strut; 16—Pin shaft; 17—Connecting rod; 18—Wire spring self-locking mechanism; 19—Rack; 20—Rack compression spring

Fig.2 Mechanism principle diagram of the movable handrail

tangent to the movable clamp is gradually away from the center of the rotating shaft. At the same time, the movable clamp approaches the fixed clamp, tightens the extravehicular fixed handrail, and realizes the stable connection with the extravehicular fixed handrail. When the astronaut presses the pawl to unlock the fixed clamping component and turns the eccentric cam in reverse, the movable clamp is separated from the fixed clamp by the spring force, which realizes the rapid separation from the extravehicular fixed handrail. The angle adjusting component follows the working principle of universal joint and cogging linkage. In the angle adjusting component, the supporting rod and the adjusting seat can rotate around the axis of the outer rod, and the base of the adjusting seat is pressed and locked by screw thread. One end of the connecting rod is connected to the pin shaft. The other end can slide along the adjusting seat and be inserted into the rack tooth slot to lock the connecting rod. The astronaut can rotate the rack, connecting rod and supporting rod to adjust the direction of the handrail, and realize the angle tilt along the connecting rod direction. The length adjusting component is designed following the principle of bevel clamping and ballpoint pen self-locking mechanism. The inner rod can slide along the inner cavity of the outer rod, and the length of the gear can be adjusted and locked through the bevel clamping and the ballpoint pen self-locking mechanism.

2 Parameter Design

The extravehicular movable handrail has complex configurations and rich functions. Many buttons and levers need to be operated by astronauts during extravehicular activities. When astronauts wear extravehicular spacesuits during extravehicular activities, they are unable to feel the external force like bare hands on the ground, nor can they exert too much operating force[10-11]. When the control switch operation force is too large, the astronauts cannot carry out the switch operation. When the force is too small, the astronauts cannot feel the switch state feedback. In order to achieve a comfortable feeling of operating force, it is necessary to design parameters of the operating force for each operating component.

2.1 Design principle and method

On the basis of the product configuration, the detailed parameter design of each operating component is carried out. The design process involves astronaut operation mode, functional constraints, working conditions and other factors. To meet the requirements of functional performance, operability and environmental adaptability, the detailed parameters and spring stiffness are calculated. According to the astronaut operation mode, the operation force and moment are checked to see if they are consistent with the force characteristics of the astronaut wearing gloves. Finally, the optimal design parameters are obtained. The specific process is shown in Fig.3.

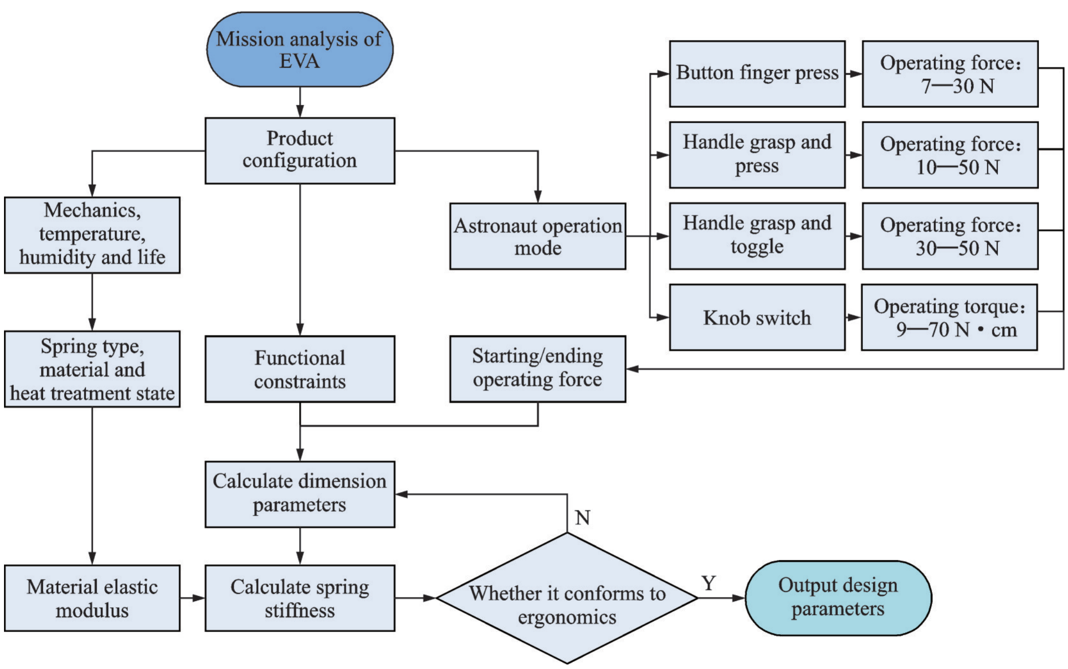

Fig.3 Operating force/moment design flow

2.2 Fixed clamping operating force

According to the motion principle of eccentric cam mechanism, the cam rotation angle φ can be taken as the independent variable to calculate the operating force. The rotation angle can be divided into two ranges with [0°, 80°] and (80°, 90°]. When the rotation angle φ varies linearly in the range of [0°, 80°], the eccentric cam pushes the movable clamp to realize the closure of the fixed clamping mechanism, as shown in Fig.4(a). When the rota-

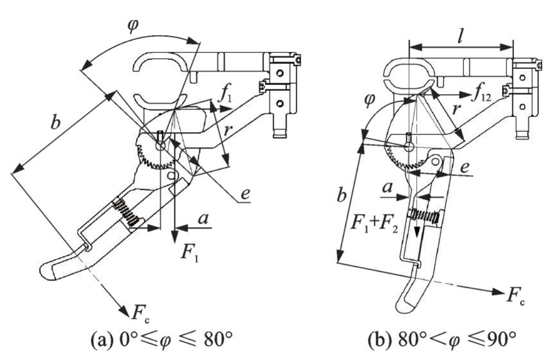

Fig.4 Operating force analysis of fixed clamping component

tion angle φ varies linearly in the range of $(80°, 90°]$, the eccentric cam pushes the movable clamp to tighten the fixed handrail of space station, as shown in Fig.4(b). In Fig.4, r is the radius of cam arc, e the eccentricity, a the magnifying force arm, b the operating force arm, F_c the fixed clamping operating force, F_1 the spring force, and F_2 the pressing force.

The operating force F_c of the fixed clamping component can be formulated as follows

$$F_c=\begin{cases} a\times(k_c\times r\times\sin(\varphi-a\sin(e\times\sin(180°-\varphi)/r))/\sin\varphi)/b & 0°\leqslant\varphi\leqslant 80° \\ a\times(k_c\times r\times\sin(\varphi-a\sin(e\times\sin(180°-\varphi)/r))/\sin\varphi+3\times E\times I\times f/l^3)/b & 80°<\varphi\leqslant 90° \end{cases} \quad (1)$$

where f is the pressing depth, E the elastic modulus, I the section inertia moment, and k_c the stiffness of pawl spring. According to the clamping principle and configuration of the fixed clamping component, the astronauts use the handle of the eccentric cam to turn the eccentric cam. Under this mode of operation, the range of operating force that the astronauts can exert is 30 N to 50 N[12-14]. The materials used for fixing clamp and movable clamping are TC4 titanium alloy. The extravehicular fixed handrail of China space station is made of 2A12 aluminum alloy. The static friction coefficient between the two materials is about 0.2[15]. When the astronaut wears pressurized extravehicular spacesuit, the maximum applied force on the palm of hand is about 88 N[16-17]. Thus, when the fixed clamping component clamps the fixed handrail of the space station, it is required to be able to withstand the static friction force of no less than 88 N along the direction of the fixed handrail. Thus, the design value of the pressing force F_2 should not be less than 440 N. Considering the calculation formula of the fixed clamping operating force, the design parameters of the fixed clamping component can be obtained, as shown in Table 1.

Table 1 Design parameters of fixed clamping component

Design parameter	Value
f/mm	0.5
e/mm	34.5
k_c/(N•mm^{-1})	1
r/mm	54.5
Augmentation ratio b/a	16

2.3 Angle adjusting operating force

In order to facilitate the astronauts to grasp the auxiliary handle in different positions, the extravehicular movable handrail is designed to possess the angle adjustment function. The angle adjusting component is composed of universal joint, linkage mechanism, friction self-locking mechanism and wire spring self-locking mechanism. The angle between the length adjusting component and the fixed clamping component can be adjusted by the universal joint. The linkage mechanism and friction self-locking mechanism can lock the axial and linkage direction angle state. The operating force of the linkage mainly overcomes the spring force of the wire spring self-locking mechanism. The wire spring self-locking mechanism is designed following the principle that the wire spring moves along the "cardioid" slot to realize the locking of the button state. The unlocking state, critical state and self-locking state of the wire spring self-locking mechanism are shown in Figs.5(a—c), respectively. In Fig.5, x_a is the pressing depth, L the wire spring length, δ_1 the "cardioid" angle, δ_2 the "half-cardioid" angle, and F_z the spring force of the wire spring.

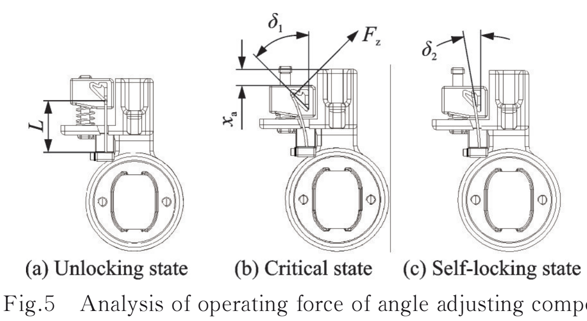

Fig.5 Analysis of operating force of angle adjusting component

The angle button unlock operating force F_{a1} can be calculated by

$$F_{a1}=\begin{cases}(k_a+3\pi Ed^4\tan\delta_1\sin\delta_1/(64L^3))x_a \\ \qquad 0\text{ mm}<x_a<10\text{ mm} \\ k_a x_a \qquad x_a=10\text{ mm}\end{cases} \quad (2)$$

The angle button lock operating force F_{a2} can be calculated by

$$F_{a2}=\begin{cases} k_a x_a & 0\ \text{mm}<x_a\leqslant 9\ \text{mm} \\ (k_a+3\pi Ed^4\tan\delta_2\sin\delta_2/64L^3)x_a & 9\ \text{mm}<x_a\leqslant 10\ \text{mm}\end{cases} \tag{3}$$

where d is the wire spring diameter and k_a the stiffness of rack spring according to the shape size and movement principle of the angle button which the astronauts operate by index finger pressing. Under this mode of operation, the astronaut's index finger can exert a pressing force of 7—30 N[12-14]. In order to satisfy that the wire spring can slide smoothly along the "heart-shaped" groove, the component force of the wire spring force in the direction of the angle button movement should be less than the horizontal lateral pressure. Considering the structural size and space constraints, the "cardioid" angle δ_1 cannot be too small. Thus, the design parameters of the angle adjusting component can be obtained, as shown in Table 2.

Table 2 Design parameters of angle adjusting component

Design parameter	Value
$\delta_1/(°)$	45
$\delta_2/(°)$	10
d/mm	1.2
L/mm	32.5
$k_a/(\text{N}\cdot\text{mm}^{-1})$	0.6

2.4 Length adjusting operating force

For the on-orbit maintenance tasks of some large extravehicular equipment, the astronauts need to carry out maintenance operations at different locations from the cabin surface. That means the position of the auxiliary handle should be adjustable. Therefore, the extravehicular movable handrail is designed to possess the length adjustment function. The length adjusting component is composed of telescopic rod, bevel pin mechanism, and bevel pin self-locking mechanism. The bevel pin mechanism uses the bevel principle to transform the vertical downward pressure of the length button into the horizontal sliding force of the bevel pin. The self-locking mechanism of bevel pin adopts the gear changing principle of deep/shallow slots to realize the locking of adjusting state. The bevel pin mechanism includes one transverse pressure spring, and the bevel pin self-locking mechanism contains two longitudinal pressure springs, which form a spring parallel system. The opening and locking states of the length adjusting component are shown in Figs.6(a, b). Among them, Spring 1 is used to realize the separation of upper and lower tooth surfaces when changing teeth, Spring 2 ensures that the lower tooth surface is alternately meshing with deep/shallow tooth surfaces, and Spring 3 provides spring back force for the bevel pin, where x_l is the longitudinal displacement, γ the bevel angle, and F_x the beveling force.

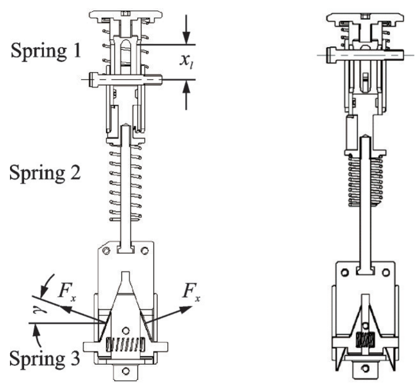

Fig.6 Analysis of operating force of length adjusting component

The length adjustment operating force F_l is formulated as follows

$$F_l=\begin{cases} k_1x_l & 0\ \text{mm}<x_l\leqslant 1\ \text{mm} \\ (4k_3\tan\gamma\cos(90°-\gamma)/\cos\gamma+k_1+k_2)x_l & 1\ \text{mm}<x_l<13\ \text{mm} \\ k_1x_l & x_l=13\ \text{mm}\end{cases} \tag{4}$$

where k_1 is the stiffness of Spring 1, k_2 the stiffness of Spring 2, and k_3 the stiffness of Spring 3. According to the working principle of the length adjusting component, the astronaut's operation mode is finger pressing. Under this mode of operation, the astronaut's fingers can exert an operating force of 7—30 N[12-14]. At the same time, in order to satisfy that the bevel pin can change the vertical force into a horizontal force, the bevel angle γ should not be greater than 45°. In addition, the horizontal sliding range of the bevel pin shall not be less than the wall thickness of the telescopic rod (4 mm). According to the trigonometric function transformation, the bevel angle γ should not be less than 17°. By comprehensively optimizing the structural size, the design parameters of the length adjusting component are obtained, as shown in Table 3.

Table 3 Design parameters of length adjusting component

Design parameter	Value
γ/(°)	20
k_1/(N•mm^{-1})	0.1
k_2/(N•mm^{-1})	0.7
k_3/(N•mm^{-1})	0.5

3 Performance Simulation Analysis

3.1 Dynamic simulation analysis of driving force

In order to verify the motion and dynamic characteristics of the designed extravehicular movable handrail, the dynamic simulation analysis of fixed clamping mechanism, angle adjusting mechanism, and length adjusting mechanism are performed with ADAMS software. The rotational driving is applied to the rotation center of the fixed clamping mechanism. The displacement driving is applied to the button of the angle-adjusting mechanism and length-adjusting mechanism.

The hand driving moment and clamping force of the fixed clamping component are shown in Fig.7. When the cam rotation angle is 0°—80°, the hand driving moment of the fixed clamping mechanism increases wavily with the cam rotation angle. The reason is that with the increase of the cam rotation angle, the distance between the rotation center of the cam and the movable clamp contact point increases. As a result, the movable clamp gradually lengthens the tension spring. In addition, when the cam rotation angle is increased by 10° every time, the pawl will cross a ratchet tooth. This is the reason for multiple peaks in the hand driving moment curve.

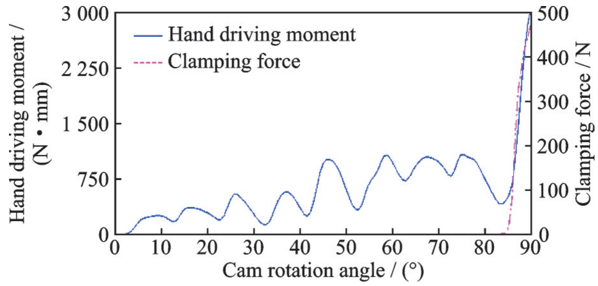

Fig.7 Analysis of hand driving moment and clamping force of fixed clamping component

When the cam rotation angle is 80°—90°, the hand driving moment rapidly increases with the increase of the cam rotation angle. The reason is that the movable clamp begins to tighten the fixed handrail, causing a rapid increase in contact force. According to the structural size of the cam, the distance between the grip area of the astronaut's hand and the center of the eccentric cam is 100 mm. Therefore, the maximum force exerted by the hand is 30 N, which is consistent with the force characteristics of the astronaut wearing gloves. From the clamping force curve, it can be seen that when the cam angle is between 80° and 90°, the clamping force increases sharply with the cam rotation angle. When the cam rotation angle is 90°, the clamping force reaches a maximum of 460 N.

As shown in Fig.8, the longitudinal displacement of the length adjusting button is driven as shown by the dotted line. The unlocking and locking process is shown in the first 2 s and the last 2 s. The length adjustment driving force curve is shown by the solid line in the figure. The driving force basically increases with the increase of longitudinal displacement. In the process of unlocking and locking, the lower tooth surface undergoes reciprocating transformation between shallow and deep teeth,

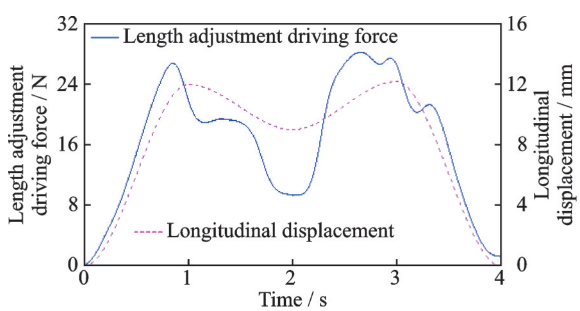

Fig.8 Analysis of length adjustment driving force

which leads to a sudden change of driving force in the process of crossing teeth.

As shown in Fig.9, the pressing depth of the angle adjustment button is driven as shown by the dotted line. The unlocking and locking process is shown in the first 2 s and the last 2 s. The angle adjustment driving force curve is shown by the solid line in the figure. When the time is 1—2 s and the pressing depth is 0—7 mm, the short edge of the wire spring slides along the inclined plane of the 45° heart-shaped chute. With the increase of the pressing depth, the bending moment of the wire spring around the z-axis gradually increases, resulting in an increase in the contact force between the wire spring and the 45° heart-shaped chute. Therefore, the angle adjustment driving force gradually increases with the increase of the pressing depth. When the pressing depth is 7.0—8.7 mm, the short edge of the wire spring slips away from the shackles of the heart-shaped groove and enters the 10° half-heart-shaped chute. The bending moment of the wire spring around the z-axis first decreases rapidly and then increases, resulting in the angle adjustment driving force first decreasing and then increasing. The maximum angle adjustment driving force is no more than 30 N. When the time is 3—4 s and the pressing depth is 0—7 mm, the bending moment of the wire spring around the z-axis is obviously weakened.

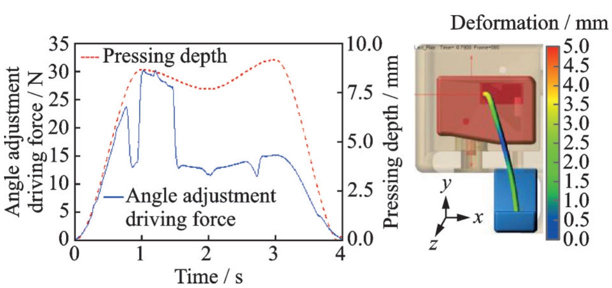

Fig.9 Analysis of angle adjustment driving force and rigid-flexible coupling dynamic model

3.2 Clamping performance simulation

According to the demand of astronauts' extravehicular operations, the auxiliary handrail is required to be able to withstand the static force of no less than 88 N in the direction of rotation around the fixed handrail. The finite element analysis method is used to simulate the static load under extreme working conditions. The maximum stress of the fixed clamping mechanism is calculated. The constitutive relation of fixed clamping mechanism parts is a bilinear isotropic strengthening model. The relationship between the extravehicular handrail and the fixed clamping mechanism is defined as friction contact. The friction coefficient is set to 0.15. In order to improve the calculation accuracy and efficiency, the augmented Lagrangian contact algorithm is adopted. The maximum moment value is 62.328 N·m under the condition of the largest angle and the longest length. The opening deformation of the movable clamping and the fixed clamping is calculated. Fig.10(a) shows the cloud image of the opening deformation of the fixed clamping mechanism and Fig.10(b) the stress cloud map of the fixed clamping mechanism.

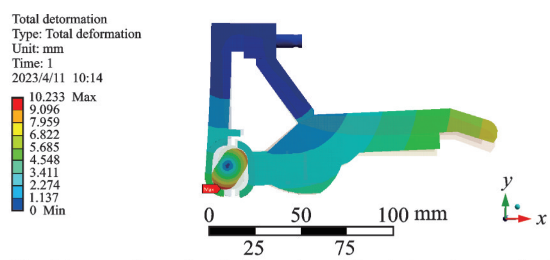

(a) Cloud image of opening deformation of fixed clamping mechanism

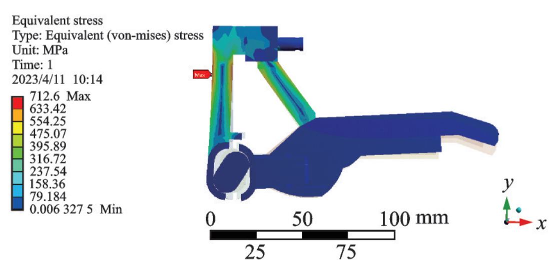

(b) Stress cloud map of fixed clamping mechanism

Fig.10 Deformation and stress cloud diagram of fixed clamping mechanism

The fixed clamping mechanism slips around the arc section of the extravehicular handrail so that the opening is enlarged with a maximum of 10.23 mm, which is less than the long edge distance of the extravehicular handrail. The maximum stress at the root of the fixed clamping is 712.6 MPa, which is less than the yield strength of TC4. The calculation results show that the deformation and stress of the fixed clamping mechanism can meet the requirements under extreme working conditions.

4 Test Verification

In order to verify the function, operating force, space environment adaptability and ergonomics characteristics of the designed extravehicular movable handrail, we carried out test verifications. The engineering prototype of the extravehicular movable handrail is shown in Fig.11.

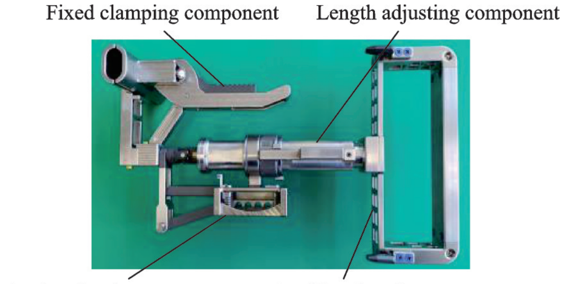

Fig.11 Engineering prototype of the extravehicular movable handrail

4.1 Verification of functional test

According to the functional requirements proposed in the design plan, the extravehicular movable handrail should have the functions of fixed clamping, length adjustment and angle adjustment. When the astronaut wears pressurized extravehicular spacesuit, the operating force of each switch needs to be in line with the force characteristics of the astronaut's hands. According to the function test of the extravehicular movable handrail, the functions of fixed clamping, angle adjustment and length adjustment can all be realized. The switching operating forces of fixed clamping component, angle adjusting component and length adjusting component are measured, respectively. The corresponding theoretical and experimental results are shown in Fig.12.

Through the theoretical curves and measured results of the operating force, we can see that the measured results are basically consistent with the theoretical curves. There is an inflection point in the operating force curve of the fixed clamping mechanism. When the rotation angle is $0^\circ \leqslant \varphi \leqslant 80^\circ$, the fixed clamping operating force varies approximately linearly with the rotation angle. The reason is that the operating force is mainly used to overcome the pulling force of the tension spring. When the rotation angle is $80^\circ < \varphi \leqslant 90^\circ$, the moving clamp begins to tighten the extravehicular handrail, resulting in a sharp increase in operating force with the increase of cam rotation angle. The operating force of angle and length adjustment increases linearly with the increase of the pressing depth and the longitudinal displacement.

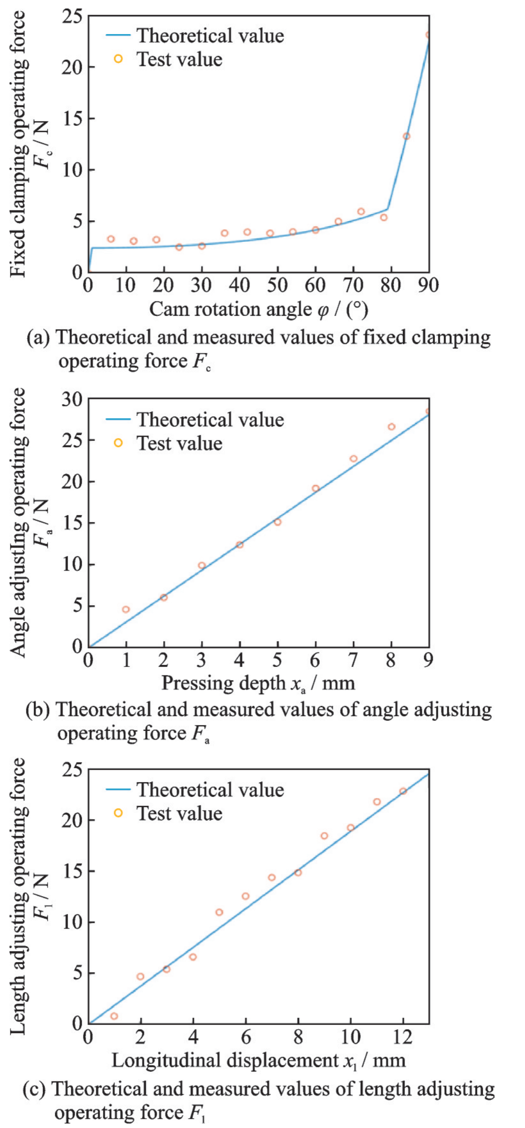

Fig.12 Theoretical and measured values of operating force

4.2 Verification of mechanical environment test

The extravehicular movable handrails will withstand various mechanical environments induced during the rocket launch[18-19]. Therefore, in order to verify the mechanical environment adaptability of the extravehicular movable handrail, we carry out the impact, sinusoidal and random vibration tests. We test the operating forces of the extravehicular movable handrail before and after the impact, sinusoidal and random vibration tests, respectively. The results are shown in Fig.13.

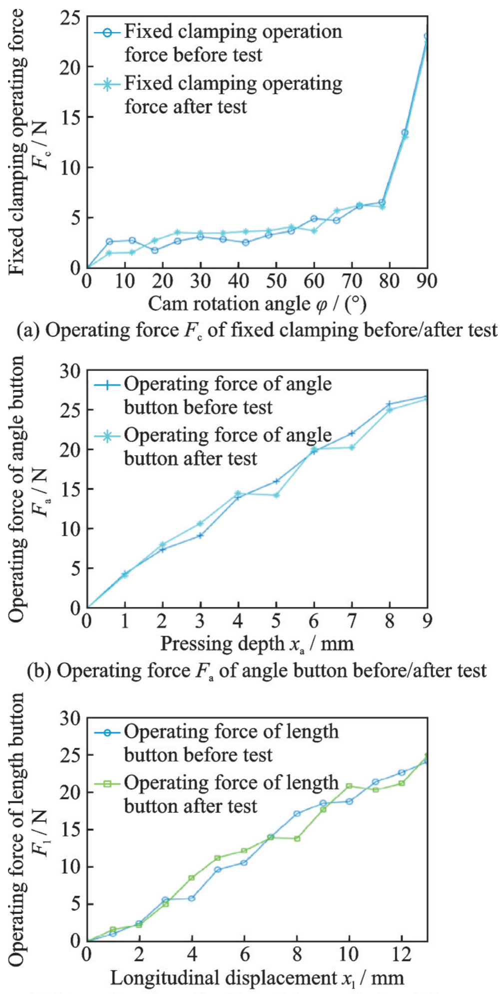

(a) Operating force F_c of fixed clamping before/after test

(b) Operating force F_a of angle button before/after test

(c) Operating force F_l of length button before/after test

Fig.13 Operating forces before/after test

As shown in Fig.13, the operating forces of the fixed clamping, angle adjusting button, and length adjusting button do not change too much before and after the test on impact, sinusoidal and random vibration. These results demonstrate that the designed extravehicular movable handrail meets the requirements of the mechanical environment.

4.3 Verification of thermal vacuum environment test

During the extravehicular maintenance mission, the temperature of the extravehicular movable handrail can vary with the change of lighting conditions and orbital environment. The thermal expansion coefficient, internal clearance, and lubrication state of the parts in the moving mechanism will all be affected by the change of temperature, which in turn affects the working performance of the product[20-21].

Therefore, in order to accurately simulate the temperature of each part of the product in the extravehicular environment of China space station, we adopt the infrared heating cage heating method to simulate the heat flow outside the surface of the product under extreme conditions. The position of the auxiliary handle is used as the temperature control point, and the position of the fixed clamping component is used as the temperature measuring point to ensure that the temperature of each part of the product can reach the steady state under extreme working conditions. According to the working performance of the spacesuit, the maximum time of a single extravehicular activity of astronauts is 7.5 h[22]. During the period, China space station orbited the Earth five times, experiencing dark areas and light areas five times with each lasting 45 min[23]. The ambient temperature of the extravehicular movable handrail changes periodically with the position of China space station around the Earth. Therefore, it is necessary to carry out the thermal cycle test. The test state is shown in Fig.14. The test temperature is the limit temperature range of the space station orbit, that is, −100—100 ℃. The number of thermal cycles is 6.5.

During the thermal vacuum cycle tests, the press operation forces of the fixed clamping component, the length adjustment button, and the angle adjustment button of the movable handrail are tested. The operating force test results of the fixed clamping component under high and low temperature conditions are shown in Figs.15(a, b). The press operation force test results of the length adjustment button under high and low temperature conditions are shown in Figs.15(c, d). The press operation force test results of the angle adjustment button under high and low temperature conditions are shown in Figs.15(e, f).

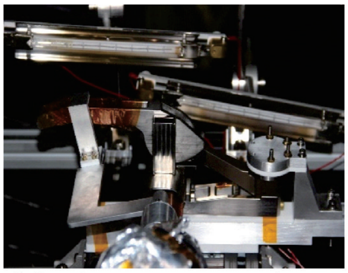

(a) Fixed clamping component eccentric cam rotation

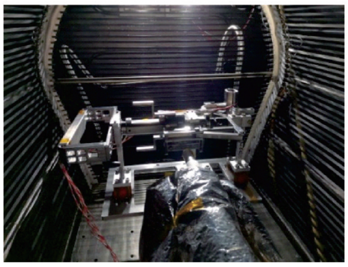

(b) Pressing the angle adjustment button

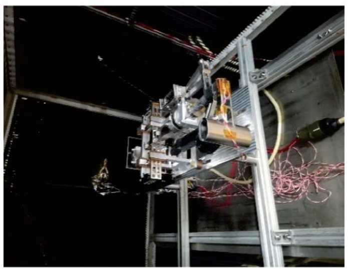

(c) Pressing the length adjustment button

Fig.14 Thermal vacuum environment test

From Fig.15, it can be seen that the operating force of the fixed clamping, the angle adjustment and the length adjustment under high temperature condition has almost no change from that under nor-

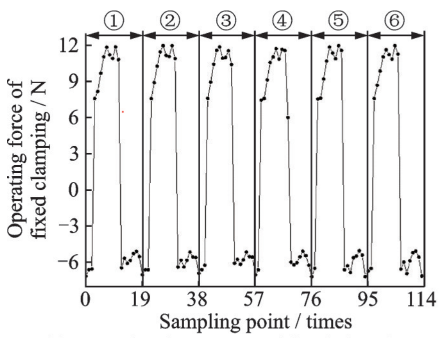

(a) Operating force curve of fixed clamping under high temperature vacuum condition

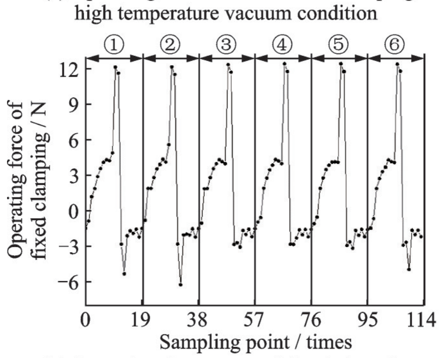

(b) Operating force curve of fixed clamping under low temperature vacuum condition

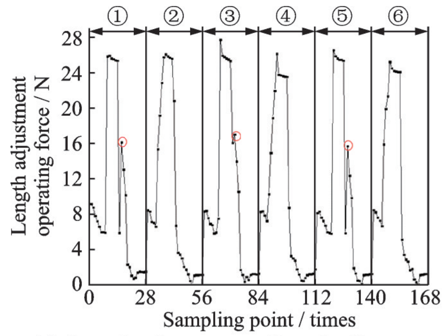

(c) Operating force curve of length adjustment under high temperature vacuum condition

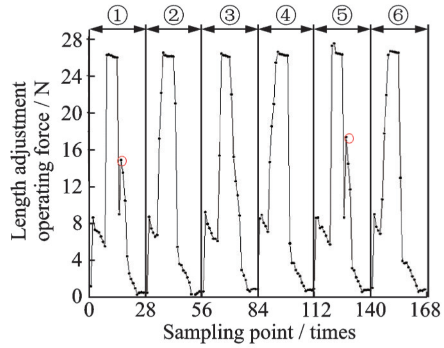

(d) Operating force curve of length adjusting under low temperature vacuum condition

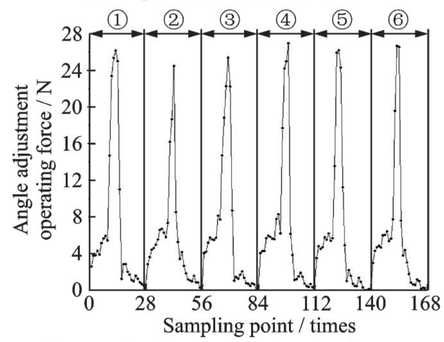

(e) Operating force curve of angle adjustment under high temperature vacuum condition

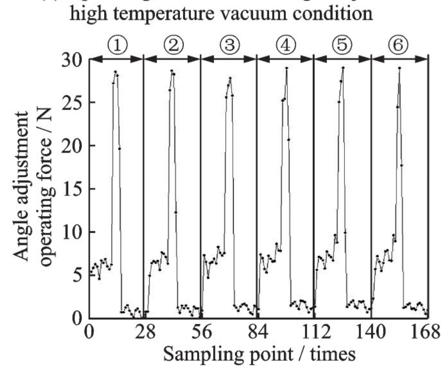

(f) Operating force curve of angle adjustment under low temperature vacuum condition

Fig.15 Operating force curves under high/low temperature vacuum conditions

mal temperature condition. At low temperature, the spring steel wire appears cold brittleness, the spring stiffness increases, and the operating force increases slightly, but it still conforms to the force application characteristics of astronauts in EVA. There are outliers in the operating force of length adjustment, which are caused by the instantaneous impact during the gear changing process of the mechanism. The results of thermal vacuum tests verify that the functions and performance of the movable handrail meet the requirements of the thermal vacuum environment.

4.4 Verification of ergonomic test

In order to verify whether the designed extravehicular movable handrail can meet the ergonomic requirements of astronauts in EVA, we check the involved ergonomic items one by one and establish an ergonomic evaluation item matrix, as shown in Table 4.

Table 4 Ergonomic evaluation items of extravehicular movable handrail

Suspension(○) / Water tank(△)	Visible & accessible	Operating alignment	Operating feedback	Operating space	Operating mode	Shape & size	Operating force
Clamping operation	△	○	○	△	○	○/△	○
Angle adjustment	△	○	○	△	○	○/△	○
Length adjustment	△	○	○	△	○	○/△	○
Product interface security (rounded corners), identification (on/off light contrast)						○	

For each evaluation item in the table, we carry out the simulated water tank and suspension ergonomics tests, as shown in Fig.16. The test results show that the operation items related with our designed extravehicular movable handrail meet the relevant ergonomic requirements of the space station.

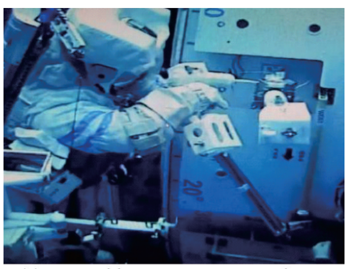
(a) Neutral buoyancy water tank test

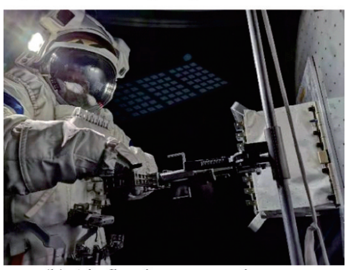
(b) Air floating suspension test

Fig.16 Ergonomic tests of weight-loss water tank and suspension

As shown in Fig.16(a), the simulated lightweight space station module with the extravehicular equipment and the hatch of the airlock module is placed in the neutral buoyancy water tank. Some floats are attached to the spacesuit to counteract gravity. Similarly, the lightweight extravehicular movable handrail also uses the same method to counteract gravity. In addition, the astronaut has six degrees of freedom in water tank. Astronauts carry out the whole process simulation of the extravehicular movable handrail wearing pressurized extravehicular spacesuit in water tank. In this way, the whole extravehicular activity task can be covered. We record the astronaut's operational position and posture, then check for any movement interference during the operation process. After the astronaut completes the entire experiment and returns to the ground, we record the astronaut's operational feedback, which includes the operational visibility, space, and flow. We further divide operational feedback into three levels, including qualified, barely qualified, and unqualified. If any item is not qualified, it is considered that the engineering prototype does not meet the ergonomic requirements.

As shown in Fig.16(b), taking the ergonomic suspension test of thermal control equipment as an example, a thermal control simulated equipment and the extravehicular handrails in the nearby area are installed on the simulated cabin board. The spacesuit is suspended by an air-floating platform. With the assistance of testers, the spacesuit can move freely in both horizontal and vertical directions. Similarly, the extravehicular movable handrail also uses the same method to counteract gravity. The movable handrail can be made of titanium alloy material in the suspension experiment. Therefore, the feedback on the operating force of each button is more accurate and the operational position and posture of astronauts can be recorded more accurately. In addition, under different light intensities, astronauts look at operation signs to simulate the working conditions in shaded areas.

5 Discussion

Because the theoretical operating force equation of the fixed clamping mechanism is calculated according to the working condition of the astronaut pressing the pawl, there is no wave peak in the theoretical operating force curve. Compared with the maximum operating force, the intermediate peak is negligible. In addition, the fixed clamping mechanism has nine gears, which is helpful to hold objects of different thicknesses during on-orbit maintenance missions.

Both the angle and length adjusting mechanisms can self-lock by changing the chute. According to the operating force curve of the test, the operating force curve of the length adjusting mechanism is smoother than that of the angle adjusting mechanism. Due to the fact that the wire spring of the angle adjusting mechanism is sensitive to temperature, there is a sudden change in the measured operating force curve. During the operation of the angle adjustment mechanism, the astronaut's fingers will feel the impact caused by the sudden change of force value.

The operating mechanism in this paper covers a variety of typical operational conditions of on-orbit maintenance of the China space station. When designing structural dimensions and spring parameters, the design parameter is obtained by the operating mode and force of astronauts wearing pressurized spacesuits. Therefore, the operational mode and force can be taken as the important input conditions, and the operational force formula can be established according to the above operating conditions. The operational force of the astronaut's hand is calculated by the operational force formula. Guide the maintenance mission procedures according to the calculated operational force.

For the scheme iteration and optimal design of the new generation of extravehicular tools, the design parameters of the prototype can provide a set of rapid design methods of clamping and adjustment. It could provide some technical references for developing and using new extravehicular tools.

6 Conclusions

(1) A novel extravehicular movable handrail for extravehicular activities of astronauts is proposed. The movable handrail is composed of fixed clamping component, angle adjusting component, length adjusting component, and auxiliary handle. The adjustable function of angle and length increases the range of astronaut activities. It provides a new design idea for the extravehicular handrail.

(2) Based on the ergonomics theory, we summarize different operating modes and the required operating forces of astronauts. Then, we quantitatively design the operating forces of each operating component, and the stiffness of the spring and structure dimensions are obtained.

(3) The dynamics analysis model of each operating component is established, and the motion range of each operating component is obtained as driving conditions. The dynamic result shows that the clamping force of the fixed clamping component can reach 460 N and the operating force is not more than 30 N.

(4) The prototype of the extravehicular movable handrail is developed. The functional, mechanical, and thermal vacuum environment tests are conducted. Specifically, during the environmental experiment, we measure the operating force. The measurement results indicate that there is no jamming during the operation process, which means that the operating force will not increase significantly due to the thermal vacuum environment.

(5) To verify the operational performance of the extravehicular movable handrail, astronauts wearing a pressurized spacesuit operate the movable handrail in the neutral buoyancy water tank test and air floating suspension test, respectively. The test covers all operations within EVA mission profile.

The test results show that the operation items related with our designed extravehicular movable handrail meet the relevant ergonomic requirements of the space station. The designed movable handrail can assist astronauts in complex extravehicular tasks.

References

[1] KAGEY R, PATTERSON L P, WILSON J L. International space station maintenance & repair group (MRG) in-flight maintenance book[M]. [S.l.]: NASA, 2000.

[2] LI Xiaodan, ZHANG Chengyu, LIANG Yingbin, et al. Review on research progress in standardization of international space stations[J]. Journal of Nanjing University of Aeronautics & Astronautics, 2021, 53 (S1): 143-147. (in Chinese)

[3] JAIRALA J C, DURKIN R, MARAK R J, et al. Extravehicular activity development and verification testing at NASA's neutral buoyancy laboratory: AIAA-2012-3592[R]. [S.l.]: AIAA, 2012.

[4] NEWMAN D, SCHMIDT P, RAHN D. Modeling the extravehicular mobility unit (EMU) spacesuit: Physiological implications for extravehicular activity (EVA) : SAE Technical Paper[R]. [S.l.]: SAE, 2000.

[5] LYNDON B. EVA tools and equipment reference book[M]. Houston Texas, USA: Johnson Space Center, 1993.

[6] STUBBINGS N B. Space station construction: The shape of spacewalks 2000—2010[C]//Proceedings of AIAA Space 2000 Conference and Exposition. Long Beach, CA, USA: AIAA, 2000.

[7] HARLAND D M. The story of space station MIR [M]. Chichester: Springer Science & Business Media, 2007: 244-247.

[8] NAN Jianghong, SHI Xueli, SHI Tongwu, et al. Thermal design and simulation analysis of space frame antenna used on China's space station[J]. Spacecraft Environment Engineering, 2021, 38(6): 625-631. (in Chinese)

[9] ZHANG Wanxin, LIAO Qianfang, LI Jinlin, et al. System design and verification of the space station Feitian extravehicular activity spacesuit[J]. Scientia Sinica (Technologica) , 2022, 52(9): 1393-1415. (in Chinese)

[10] ZHOU Qianxiang, CHEN Ling. Advances of studies on ergonomic design of man-machine interface in extravehicular operation[J]. Chinese Journal of Aerospace Medicine, 2004, 15(3): 184-187. (in Chinese)

[11] CHEN Jindun, ZHAI Zhihong, FU Yuanhua, et al. Verification items and methods for EVA in China space station[J]. Manned Spaceflight, 2019, 25(6): 733-739. (in Chinese)

[12] MATTY J. Results and analysis from spacesuit joint torque testing[C]//Proceedings of the 40th International Conference on Environmental Systems. Barcelona, Spain: AIAA, 2010.

[13] Institute of Space Medico-Engineering. Ergonomic requirement and evaluation method for spacecraft engineering design by astronaut system: GJB6765—2009 [S]. Beijing: General Equipment Headquarters of PLA, 2009. (in Chinese)

[14] Office of the Chief Health and Medical Officer. NASA spaceflight human-system standard: NASA-STD-3001(Volume 1)[S]. [S.l.]: NASA, 2007.

[15] Office of the Chief Health and Medical Officer. NASA spaceflight human-system standard: NASA-STD-3001 (Volume 2)[S]. [S.l.]: NASA, 2011.

[16] TILLMAN B, TILLMAN P, ROSE R R, et al. Human factors and ergonomics design handbook[M]. [S. l.]: McGraw-Hill Education, 2016.

[17] CHEN Xi, CUI Liguo. Paper and board—Determination of the static and kinetic coefficients of friction—Horizontal plane method: GB/T 22895—2008[S]. Beijing: Standardization Administration of the People's Republic of China, 2008. (in Chinese)

[18] TIAN D K, GUO Z W, JIN L. Design and mechanical characteristics of support structure for modular deployable antenna[J]. Transactions of Nanjing University of Aeronautics and Astronautics, 2023, 40(1): 80-97.

[19] MA Xingrui, HAN Zengyao, ZOU Yuanjie, et al. Review and assessment of spacecraft mechanical environment analysis and specification determination[J]. Journal of Astronautics, 2012, 33(1): 1-12. (in Chinese)

[20] LIU Shengli, WANG Xingdong, KONG Jianyi, et al. Kinematic reliability analysis of planar metamorphic mechanism with multi-source uncertainties[J]. Journal of Mechanical Engineering, 2021, 57(17): 64-75. (in Chinese)

[21] ZHANG Zhengyao, JIANG Shichen, WANG Meng, et al. Analysis of influencing factors on thermal deformation of satellite onboard antenna reflector[J]. Spacecraft Environment Engineering, 2021, 38(2): 130-137. (in Chinese)

[22] BOWMAN R, BACHLE S, DODD T, et al. NASA's development of next-generation spacesuits:

NASA 1G-21-025[R]. [S.l.]: NASA, 2021.

[23] LIU Yinhua, CHEN Ruiqiong, LIU Ya, et al. Common-view differences between space station and GNSS and accuracy analysis[J]. Journal of Astronautics 2022, 43(10): 1389-1398. (in Chinese)

Acknowledgements This work was supported by the CAST Science Foundation for Distinguished Young Scholars of China (No.R-WY-JQRC-19). The authors would like to acknowledge the following people for their assistance: Dr. TAN Lifen and Mr. ZHAO Yang with the National Key Laboratory of Human Factors Engineering, Astronaut Center Of China; Dr. LI Fangyong and Mr. GUO Wei with the National Key Laboratory of Science and Technology on Reliability and Environmental Engineering Technology, Beijing Institute of Spacecraft Environment Engineering.

Authors Mr. **LIU Junliang** received the M. S. degree in mechatronics engineering from Harbin Institute of Technology, Harbin, China, in 2016. He joined Beijing Institute of Spacecraft Environment Engineering in April 2020. His research interests include on-orbit maintenance technology of spacecraft, such as extravehicular maintenance technology for manned spacecraft, end actuators of space robot and auxiliary equipment for manned lunar landings.

Prof. **FU Hao** received the Ph.D. degree in mechatronics engineering from Harbin Institute of Technology, Harbin, China. He is in charge of extravehicular maintenance tools of China Space Station. He is the director of Beijing Aerospace Products Intelligent Assembly Technology and Equipment Engineering Technology Center. He won model worker of China Aerospace Science and Technology Corporation. His research focuses on extravehicular maintenance technology for manned spacecraft, satellite automatic production and thermal control technology for satellites.

Author contributions Mr. **LIU Junliang** designed the models, conducted the analysis, interpreted the results and wrote the manuscript. Prof. **FU Hao** contributed to data and model components for the fixed clamping model. Mr. **WANG Zhe** contributed to data for the analysis of the operating force. Mr. **FAN Ziqi** and Mr. **GUO Tao** contributed to the discussion and background of the study. All authors commented on the manuscript draft and approved the submission.

Competing interests The authors declare no competing interests.

(Production Editor: XU Chengting)

航天员出舱活动用移动扶手原型设计与试验验证

刘俊良[1]，傅　浩[1,2]，王　哲[1]，范子琦[1]，郭　涛[1]

(1.北京卫星环境工程研究所，北京 100094，中国；2.哈尔滨工业大学机电工程学院，哈尔滨 150001，中国)

摘要：针对空间站舱外固定扶手难以满足航天员复杂舱外作业需求的问题，提出一种航天员出舱活动用的移动扶手，并对其进行了参数设计与试验研究。首先，在充分考虑着舱外服加压航天员手部施力特性的基础上，对舱外移动扶手操作机构的几何尺寸和弹簧刚度进行了参数设计。其次，为满足航天员在轨出舱单手操作移动扶手的人机工效学需求，对操作机构进行了自锁设计，并利用ADAMS对操作机构进行了动力学仿真分析，仿真结果表明，各操作机构能够实现自锁功能，且操作力符合着服加压航天员手部施力特性。最后，研制了舱外移动扶手原理样机，从功能、环境适应性及人机工效学方面进行了试验验证。试验结果表明：所述方案可顺利完成舱体扶手夹持、长度和角度调节，且实测操作力与理论值基本吻合，在力学和热学环境试验前后操作力无明显变化，各操作机构满足空间站舱外低轨环境及人机工效学要求。

关键词：出舱活动；出舱移动扶手；机构设计；人机工效学